ORIGINAL PAPER

Evaluation of electrospun nanofibers fabricated using PCL/PVP and PVA/β-TCP as potential scaffolds for bone tissue engineering

Majid Sohrabi[1] · Marjan Abbasi[1] · Malek Masoud Ansar[2] ·
Bahram Soltani Tehrani[3]

Abstract

In order to create a perfect bone scaffold, nanocomposites are the best options, as they can be engineered to have the composition, structure and properties of natural bone. In the present study, the layer-by-layer and hybrid nanofiber scaffold are fabricated by electrospinning method using a combination of PCL/PVP and PVA/β-TCP layers. We study and compare the morphological properties (scanning electron microscope (SEM), swelling ratio and porosity), mechanical properties (tensile strength, elongation at break and tensile modulus) and biodegradability of the scaffolds. The average fiber diameter measured for layer-by-layer and hybrid scaffolds is 446 ± 128 nm and 505 ± 261 nm, respectively. The tensile strength for the layer-by-layer and hybrid scaffolds is 7.40 ± 3.40 MPa and 6.57 ± 1.64 MPa, respectively, and the degradation rate for layer-by-layer and hybrid scaffolds is $26 \pm 2\%$ and $40 \pm 5\%$, respectively. So the results show the desired mechanical properties and compatibility of scaffolds. The (3-(4,5-dimethylthiazol-2-yl)-2,5-diphenyltetrazolium bromide) (MTT) assay shows cell viability above 80% and absence of cell cytotoxicity for layer-by-layer and hybrid scaffolds after 3, 5 and 7 days of rat marrow stromal cell (rMSC) culture. The morphology and proliferation of rMSC cells show the suitability of the scaffolds for tissue engineering application. Therefore, both types of scaffolds can be used in several tissue engineering applications, including improvement of bone tissue regeneration.

Keywords Electrospinning · Hydrophilic polymers · Poly(ε-caprolactone) · Scaffold · Tissue · Engineering

---

✉ Marjan Abbasi
m.abbasi@guilan.ac.ir

Extended author information available on the last page of the article

Introduction

Natural bone tissue is made from a nanocomposite structure that consists of permeable polymer ceramic material, a lamellar material and a fiber matrix material. Bone tissue engineering scaffolds use a scaffold as a framework for preserving the natural elements of cells, to repair or improve bone defects [1, 2]. The perfect scaffold for tissue engineering must have mechanical and biological properties analogous to the natural bone tissues. The natural bone mainly consists of an organic matrix (collagen fibers) and an inorganic crystalline phase (nano-hydroxyapatite), which form a natural nanocomposite [3, 4].

The mechanical properties of polymeric scaffolds are not similar to the natural bone while fabricated scaffolds of inorganic materials are very fragile, making it impossible to control [5–7]. Composite scaffolds such as polymer/calcium phosphate are a good candidate for bone tissue engineering [8].

There are different types of methods for producing continuous fibers from synthetic, natural or blend polymers and inorganic materials, including electrospinning, phase separation, self-assembly, melt blowing, freeze-drying and template synthesis for targeted applications.

However, some methods are unsuitable for many polymers, or the process unmanageable, or the fiber diameter and direction are un-adjustable. As a straightforward method of fiber production, electrospinning is compatible with a variety of materials and has a variety of techniques using electrostatic forces for the production of fibers with suitable surface topography, morphology and diameter distribution of fibers to the nanoscale [9, 10].

Utilizing electrospinning, it is feasible to fabricate scaffolds that mimic the natural extracellular matrix (ECM) bone design, due to its high aspect ratio, high porosity and large surface area. The high specific surface area of the electrospun scaffolds makes more surfaces appropriate for cell adhesion, while the high porosity and the high interconnectivity of pores give sufficient capacity to the vascularization needed to support new bone and provide the swapping of nutrient and metabolic losses among the scaffold and atmosphere [11].

Tricalcium phosphate (TCP) is a bioceramic that absorbs quicker than synthetic HA but does not have its mechanical properties. There are alpha and beta crystalline forms [12]. β-TCP is favored over other TCP structures because of its great chemical stability and constant biosorption rate [13]. The β-TCP form is steadily under 1125 °C while the α-form is just steady in the scope of 1125–1430 °C. α-TCP is extremely reactive and degrades quickly in vitro, so it is not utilized as bone linkage material [14]. β-TCP has been widely used clinically since the 1970s as an artificial bone filler in the fields of dental and orthopedic medical procedures, and its biocompatibility has been corroborated in experimental evaluations. The incorporation of ceramic nanoparticles such as calcium phosphate (CaP) to polymer matrices has turned into a mainstream strategy to fabricate composite scaffolds. CaP biomaterials if fabricated with proper geometry or topography [15, 16] are bioactive and osteoconductive [17].

As a nanostructured coating, combined with a polymer matrix, CaP can enhance the mechanical properties of polymeric materials and has an effective role in enhancing cell adhesion and inducing the differentiation and proliferation of osteoprogenitor cells.

Polycaprolactone (PCL) with great mechanical properties is a biocompatible and biodegradable polyester [18]. PCL shows better mechanical quality than other bioresorbable polymeric materials and degrades at a rate suitable for bone regeneration [19, 20]. Nevertheless, PCL is inappropriate for cell attachment and proliferation because of its hydrophobic nature and poor surface wetting and insignificant reaction with biological liquids. Therefore, it is very necessary to enhance the hydrophilicity of PCL to overcome the challenges that come from its hydrophobic nature [21]. To enhance the hydrophilicity of the PCL, collagen [22] and gelatin [23] were utilized and were successful in reaching cell adhesion. Poly(vinyl pyrrolidone) (PVP) and polyvinyl alcohol (PVA) are hydrophilic polymers, were famous for their great biocompatibility with living tissue and very low cytotoxicity [24]. PVP and PVA were mixed with PCL to acquire a scaffold with favorable hydrophilicity and degradation properties [25, 26].

The present work aims to compare and evaluate layer-by-layer and hybrid nanofiber composite scaffolds, including PCL for the backbone of the scaffold and PVP with PVA to increase hydrophilicity and degradation rate and also with the incorporation of β-TCP for better mineralization. The properties of the composite scaffolds obtained were characterized by SEM, FTIR, mechanical properties, porosity, swelling and MTT methods.

Materials and methods

Materials

PCL with a molecular mass of 70,000–90,000 g/mol was purchased from Sigma-Aldrich (St Louis, MO, USA). Molecular weight of PVP and PVA was 40,000 g/mol and 72,000 g/mol, respectively, and they were purchased from Merk Chemical Co (Germany). Acetic acid (AcOH) with ≥99% purity, dichloromethane (CH_2Cl_2) with ≥99.5% purity, N,N-methylenebisacrylamide ($C_7H_{10}N_2O_2$) with ≥99% purity and ammonium persulfate ((NH_4)S_2O_8) with ≥98% purity was obtained from Merk Chemical Co (Germany). Beta-tricalcium phosphate ceramic nanoparticles (β-TCP) were produced at the Institute of Nik Ceram Razi Co by sol–gel method. All chemicals were used without further purification.

Preparation of electrospinning solutions

Figure 1 shows the schematic diagram of the electrospinning setup. The 15% (w/v) PCL solution was prepared by dissolving 0.3 g of PCL in 90% acetic acid solvent and stirred for 24 h at room temperature for homogenization. The solution of 15% (w/v) with the weight ratio of PCL/PVP (60/40) was prepared by dissolving certain amounts of

Fig. 1 Schematic of the hybrid and layer-by-layer electrospinning setup
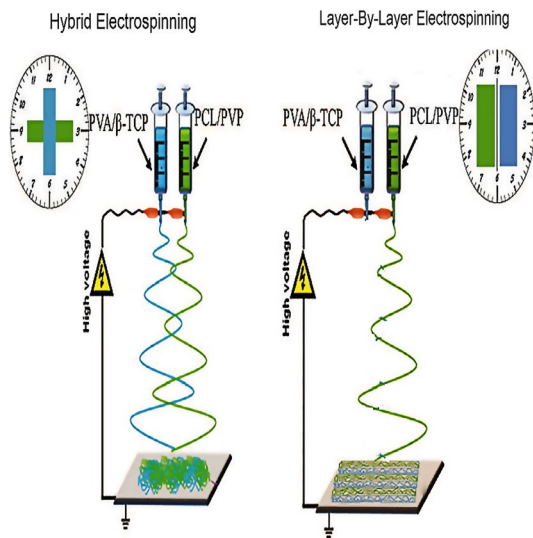
polymers in a dichloromethane (DCM) solvent and stirred at room temperature for 3 h. The solution of 12% (w/v) PVA was prepared from 0.24 g of polymer in distilled water and stirred at 70 °C for 3 h. Then, 0.012 g (β-TCP) was added into the PVA solution and sonicated. The optimum conditions for electrospinning were chosen for these solutions and their composition of the prepared samples after the trial-and-error method. Each of the prepared solutions were placed in a separate syringe for electrospinning.

Electrospinning

The provided solutions were transferred into the 5-mL plastic syringe with a syringe needle. The electrospinning conditions and prepared solutions concentration were selected after some trial and error. The high voltage connected to the needle tip was 15 kV. The flow rate was set at 0.2 ml/h by a syringe pump. Nonwoven electrospun fibers were kept onto a grounded aluminum foil as the collector was set at a fixed distance of 15 cm from the needle tip. For the electrospinning of solutions, PCL/PVP and PVA/β-TCP were placed in two separate syringes and hybrid electrospinning was performed for 3 h. To perform layer-by-layer electrospinning, each nozzle was subjected to electrospinning for 30 min and this was repeated three times for each nozzle in this method. To evaporate the remaining solvent, the nanocomposite fiber mats were dried at 37 °C for two days and then placed in a desiccator for further examinations.

Cross-linking treatment

In this study, according to the two layers used, in the layer that included PVA/β-TCP, the cross-linking agent has been used according to the following references [27, 28] which is described as follows: The cross-linking process was carried out by adding

the initiator of ammonium persulfate to the prepared solutions, and after homogenization in the stirrer, adding the *N,N*-methylenebisacrylamide to the prepared solutions and after 2 h of stirring, to fix the cross-linking process, the nanofibers were kept in the oven at 110 °C for 10 min. The layer that included PCL/PVP, with the presence of PCL that is a hydrophobic polymer, acts alone as the cross-linking agent. Therefore, there is no need for a cross-linking agent in this layer [29]. Finally, the validation of cross-linking treatment was checked by testing the dissolvability of the cross-linking mats immersed in phosphate-buffered solution (PBS, pH 7.4) at 37 °C for 48 h.

Characterization

The electrospun scaffold tests were sputter-coated with gold and examined by a scanning electron microscope (JEOL JSM 5500, Japan). The average diameter of the fibers was resolved by performing estimations on 50 fibers. The morphology and placement of cells on scaffolds were also carried out using SEM.

FTIR spectra were recorded using Nikolet Magan-IR 560 spectrophotometer (ATR procedure, in the 400–4000 cm^{-1} range, the Netherlands).

The water maintenance level was controlled by finding the swelling proportion for the arranged scaffolds. Firstly, the rectangular shape test was cut and plunged in deionized water for 24 h. Then the water on the sample surface was absorbed with filter paper, and the sample was weighed in wet condition. The swelling proportion was computed by the following formula:

$$\text{Swelling Ratio}\,(\%) = \frac{W_S - W_d}{W_d} \times 100 \tag{1}$$

where W_S is the sample dry weight and W_d is the sample wet weight. Each swelling test was repeated three times [30].

The porosity of the electrospun scaffolds was assessed by utilizing a gravimetric measurement. Concisely, the electrospun meshes were punched into 20 mm circles. In the wake of the measuring thickness, the volume of the scaffold could be determined. The mass of the scaffold was also measured for the density of the scaffold (ρ_{ap}). The porosity was then computed by the following formula:

$$\text{Porosity} = \left(1 - \frac{\rho_{ap}}{\rho_m}\right) \times 100\% \tag{2}$$

where ρ_m is the density of the scaffold material that included PCL, PVP and PVA with apparent density ($\rho_{ap} = 1.14, 1.20, 1.25$) g/cm^3, respectively.

Mechanical properties of the scaffolds were recorded using Sherly micro 50 fiber tensile tester. The samples with known area density were cut into strips with dimensions of 2 cm×0.3 cm and then were mounted at the tensile tester. The strain rate and gage length in the measurements were 2 mm/min and 2 cm, respectively. At least 5 samples were tested, and their load–strain curves were recorded. The results

of the tensile strength, strains and tensile modulus were averaged and reported. The max stress of the examined samples was then calculated as the following formula:

$$S = \frac{d \times B}{A \times W} \times 100 \tag{3}$$

where S is the stress in MPa, B is the breaking load in N, A is the area density in g/m^2, W is the specimen width in m and d is the density in g/cm^3. The tensile modulus of the samples was calculated from the slop of the initial parts of the load–strain curve [31].

To calculate biodegradability, the samples were submerged in PBS with the pH of 7.4 and were stirred in a water bath at 37 °C for 28 days. The samples were removed after a week and washed with purified water and dried at room temperature (27 °C, under vacuum). The change in mass due to degradation was computed utilizing the following formula:

$$\text{Weight loss}(\%) = \frac{W_i - W_f}{W_f} \times 100 \tag{4}$$

where W_i is the initial mass of the sample and W_f is the final mass of the dried sample after the degradation process [32].

Cell study

Cell viability assay

MTT (3-[4,5-dimethylthiazol-2-yl]-2,5-diphenyltetrazolium bromide; thiazolyl blue) test was used to detect toxicity or harmful reactions [33, 34]. MTT reagent is a yellow tetrazolium salt that produces a dark-blue formazan crystal when interacting with viable cells. Accordingly, the content of formazan can reflect the level of cell metabolism [35].

MTT assay was done by an ISO10993-5. Rat bone marrow mesenchymal stem cells were cultured in a DMEM medium (10% fetal bovine serum, 1.0% penicillin–streptomycin) under 37 °C in 5% CO_2. When the cells reached 70% confluence, they were trypsinized with 0.25% trypsin and 1 ml ethylenediamine tetraacetic acid. The viabilities of cells were determined by the MTT assay. For the MTT assay, the scaffolds were sterilized with extremely compressed steam for 15 min and placed in 1 mL of DMEM medium, and then incubated for 24 h at 37 °C. Rat bone marrow mesenchymal stem cells were seeded in wells of a 96-well plate at a density of 5000 cells per well. After incubation for another 24 h, the culture medium was removed and replaced with the as-prepared extraction medium and incubated for another 3, 5 and 7 days, respectively. The OD value of the formazan solution was detected by an ELISA reader (Multiscan MK3, Lab system, Finland) at 570 nm [36, 37]. The assay was performed three times for each of the scaffolds. The average of the cell viability values was compared to the control to decide the effect of the scaffold on cells, and % cell viability was plotted versus various scaffolds.

Cell morphology

The cell morphology on the scaffold was examined utilizing scanning electron microscopy (JEOL JSM 5500, Japan) working at an accelerating voltage of 5–20 kV. The cell-seeded scaffolds were washed with PBS and settled using 10% neutral formalin buffer for 5 h at 4 °C. Scaffolds were dehydrated by classified ethanol (10–100%) treatment and dried overnight. The dried composite scaffolds with cells were covered with gold for further cell morphology examined by SEM. Samples were attentively studied at lower and higher magnifications to evaluate the morphology of adhered cells.

Statistical analysis

All the experiments were performed at least three times, and the average of the results was notified as mean $\pm$ SD. Statistical calculations were performed by one-way ANOVA for all the data at a statistical significance level of $p < 0.05$.

Results and discussion

Fiber diameter and morphology

The morphology of the scaffolds along with their fiber diameter distribution is shown in Fig. 2. The nanofibers of the resulting scaffolds are formed in an interconnected network with a nonuniform morphology in some sections, but no bead is seen in the scaffolds, as shown in Fig. 2. Nanofiber diameter analysis shows that the mean fiber diameter of PCL/PVP nanofibers is 314 ± 96 nm, and the mean fiber diameter of the PVA/β-TCP nanofibers is 487 ± 123 nm. This increase in diameter in nanofibers is due to the presence of PVA with a much higher molecular weight than the PVP, as well as the presence of nanoparticles of β-TCP in the composition. The ceramic nanoparticles such as β-TC increase the viscosity of the polymer solution and improve the resistance to long elongation during electrospinning; hence, the diameter of the nanofibers increases [38].

The mean fiber diameter of the layer-by-layer and hybrid scaffolds was 446 ± 128 nm and 505 ± 261 nm, respectively. These results demonstrate the increase in the average diameter of the hybrid scaffolds compared to the layer-by-layer scaffold.

FTIR Spectroscopy

Functional groups assignments and their respective bonding interactions of scaffolds can be deduced using FTIR spectroscopy as shown in Fig. 3. The FTIR spectrum for PCL/PVP is shown in Fig. 3a and analyzed based on the characteristic bands [39]. The band at 2945 cm^{-1} and 2867 cm^{-1} corresponds to the asymmetric and
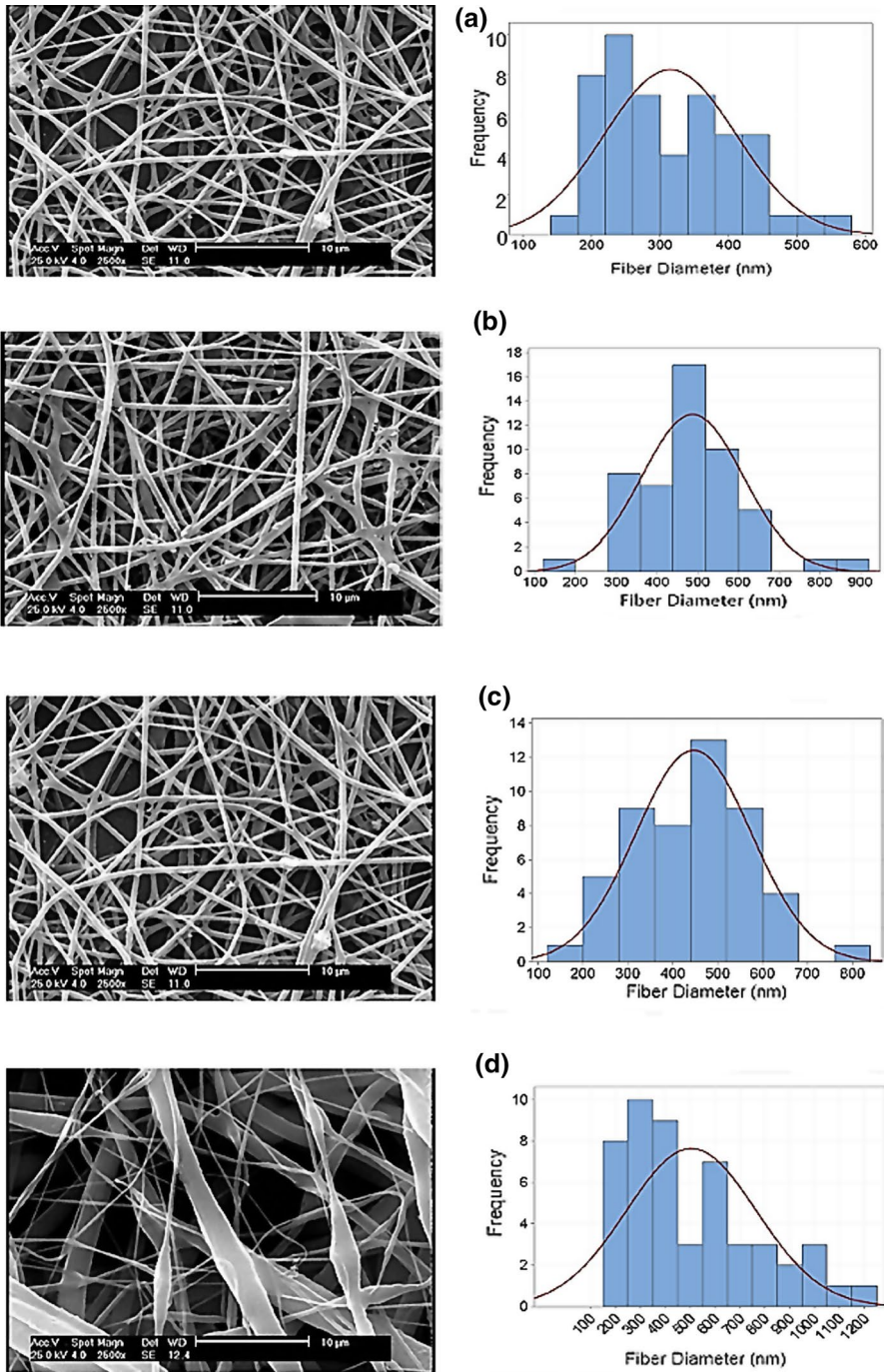
Fig. 2 SEM images of the fibrous scaffold with its diameter frequency distribution: **a** PCL/PVP; **b** PVA/β-TCP; **c** layer-by-layer; **d** hybrid

symmetric stretching vibration of C–H, respectively. The strong peak at 1725 cm^{-1} is related to the stretching vibration of the C=O ester carbonyl group in the PCL, and the absorption band at 1660 cm^{-1} was related to the stretching vibration of the C=O group in amide in PVP. Also, the peak of 1287 cm^{-1} is related to the stretching vibration of C–N in PVP and the peak of the 1057–1164 cm^{-1} for symmetric stretching vibration of the C–O–C in PCL and PVP polymers. In general, the peaks mentioned above confirm the presence of PCL and PVP polymers in the scaffold. The FTIR spectrum for PCL/PVA/β-TCP is shown in Fig. 3b and analyzed based on the characteristic bands [40]. In this FTIR spectrum, the bands at 900–1200 cm^{-1} were due to the stretching mode of the PO$_4^{3-}$ group, which is related to the TCP nanoparticles. The peak of 1722 cm^{-1} is related to the stretching vibration of the C=O ester carbonyl group, the peak of 1292–1294 cm^{-1} related to the stretching vibration of the C–O group and the peak of the 1367–1369 cm^{-1} for the C–H bending vibration, which confirms the presence of the PCL polymer in the scaffold. Also, the peak 330 cm^{-1} and 1432 cm^{-1} is related to the CH$_2$ bending, and the peak of the 3352 cm^{-1} is related to the O–H stretching vibration of the hydroxyl group of PVA.

Measurement of water swelling ratio (hydrophilicity) of prepared scaffolds

The ability to absorb water is an important factor in the substrate used in tissue engineering; in fact, water absorption reflects the ability of scaffolds to absorb extra secretions and keep the wounds moist. Additionally, hydrophilic scaffolds enhance cellular attachment and also increase the biocompatibility and proliferation of cells [40]. Electrospun scaffolds generally are very porous in nature, which adds to the content of water held inside the fibers. The swelling ratio of the scaffolds was calculated by immersion samples in the PBS. In general, materials with more hydrophilic properties have a greater ability to retain and absorb water, which is evaluated by measuring swelling ratio in materials. The variation of the

Fig. 3 FTIR spectra of electrospun scaffolds: **a** PCL/PVP; **b** PCL/PVA/β-TCP
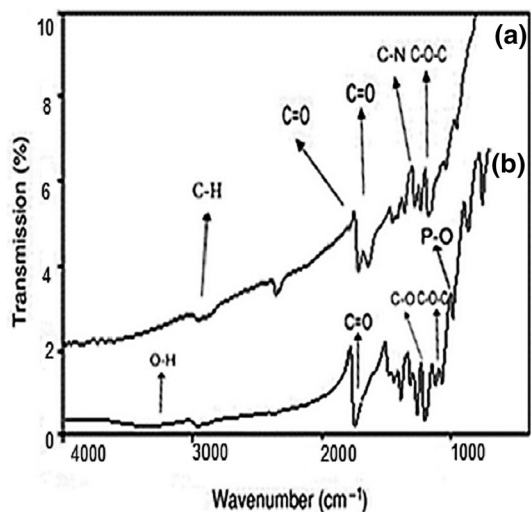
sample's swelling ratio as an indicator of the degree of hydrophilicity is shown in Table 1. Since PCL is hydrophobic in nature, the hydrophilic polymers are used to improve the hydrophilicity of the scaffolds. The swelling ratio of PCL/PVP is found at $738 \pm 162\%$, which shows that the difference is significantly higher compared to PCL ($p < 0.05$). Furthermore, the hydrophilicity of PVA/β-TCP is found to be $542 \pm 223\%$ indicating that despite benefiting from PVA, it is less hydrophilic, due to the incorporation of ceramic antiparticles cross-linking treatment compared to PCL/PVP. The swelling ratio of layer-by-layer and hybrid scaffolds was $811 \pm 214\%$ and $605 \pm 125\%$, respectively. These results indicate the hydrophilicity in the layer-by-layer scaffold is significantly higher than hybrid scaffold ($p < 0.05$). Since hydrophilicity is a more surface-s factor, it seems to be due to the fact that in the layer-by-layer scaffold, the layer included PCL/PVP is placed on its surface alone, while in the hybrid scaffold there is a combination of layers, which included PCL/PVP and PVA/β-TCP on the surface of the scaffold. According to the results, it is clear that the layer containing PCL/PVP shows higher hydrophilicity. Therefore, the average hydrophilicity in the layer-by-layer scaffold is higher than the average hydrophilicity in the hybrid scaffold.

Porosity measurement

The presence of suitable porosity within the scaffold is very important for regulating the essential processes of the nutrient reserve to cells, metabolite dispersion, local pH stability and cell signal. The size of the pores is additionally a crucial parameter to evaluate the nearness of cells in cell–cell connection in three dimensions and the space available for cells to possess a 3-D organization within the later step of tissue growth [41, 42]. Additionally, porosity can determine the kinetics of cell migration into the scaffold. Therefore, this feature is essential for the scaffold. The porosity measurement results in Table 1 show that the porosity for PCL was 69 ± 5. By adding PVP, the porosity increases to $73 \pm 4\%$. In the PVA/β-TCP, it is found to be $70 \pm 4\%$. This decrease in porosity in the presence of β-TCP as the filler may be due to the fact that the addition of β-TCP leads to a thicker wall of lower porosity. In comparison, in the layer-by-layer and hybrid scaffolds, the porosity was measured $75 \pm 5\%$ and $55 \pm 4\%$, respectively. The porosity was significantly higher in the layer-by-layer scaffold compared to the hybrid scaffold ($p < 0.05$).

Table 1 Swelling ratio and porosity of electrospun scaffolds

Scaffold	Swelling ratio (%)	Porosity (%)
PCL	–	69 ± 5
PCL/PVP	738 ± 162	73 ± 4
PVA/β-TCP	542 ± 223	70 ± 4
Layer-by-layer	811 ± 214	75 ± 5
Hybrid	560 ± 125	55 ± 4

Mechanical properties

The mechanical properties of the scaffold must be compatible with the tissue in contact with it. The desired scaffold in tissue engineering should have good mechanical properties. The mechanical properties of scaffolds are given in Table 2. The tensile strength decreases dramatically in the PCL/PVP, tensile strength of PCL and PCL/PVP found to be 10.02 ± 3.29 MPa and 2.11 ± 0.87 MPa, respectively. The tensile strength in the PVA/β-TCP was found 8.81 ± 2.83 MPa, which is justified by the cross-linking treatment and the presence of ceramic nanoparticles. The tensile strength of the layer-by-layer and hybrid scaffolds was measured, and their values were calculated 7.40 ± 3.40 MPa and 6.57 ± 1.64 MPa, respectively. The tensile strength of the scaffolds are not significantly different from each other ($p < 0.05$). Similar changes are observed in the tensile strength of the samples by adding hydrogel, ceramic nanoparticles and cross-linking treatment in the tensile modulus. The tensile modulus of layer-by-layer and hybrid scaffolds were measured 266 ± 107 and 52.6 ± 9.3, respectively. Tensile modulus in the layer-by-layer scaffold is significantly higher than hybrid scaffold ($p < 0.05$). The elongation at break of the layer-by-layer and hybrid scaffolds was measured $10 \pm 5\%$ and $68 \pm 27\%$, respectively. Results show the elongation at break in the hybrid scaffold is significantly higher compared to the layer-by-layer scaffold ($p < 0.05$).

These results show that the layer-by-layer scaffold has higher tensile strength and tensile modulus and also less elongation at break than the hybrid scaffold. The reason seems to be that the layer-by-layer scaffold has smaller mean fiber diameter and more uniform diameter distribution compared to the hybrid scaffold.

Investigation of degradation rate

The degradation rate of a scaffold is an essential parameter for tissue engineering since it should match with the rate of neogenesis of ECM. The very high rate of scaffolds degradation that is planted in the body may damage the process of cell proliferation, and also very low degradation rates may delay the process of integrating these scaffolds with the surrounding tissue [43]. Accordingly, the vitro biodegradation was studied by evaluating the weight loss of the scaffolds in PBS at the temperature of 37 °C in the span of 4 weeks. The biodegradability of the scaffolds in Fig. 4 shows that the PCL degradability is negligible after 28 days,

Table 2 Mechanical properties of electrospun scaffolds

| Scaffold	Tensile strength (MPa)	Elongation at break (%)	Tensile modulus (MPa)
PCL	3.29 ± 10.02	3.5 ± 27	77 ± 30
PCL/PVP	2.11 ± 0.87	20 ± 61	3.62 ± 8.73
PVA/β-TCP	8.81 ± 2.83	4.70 ± 9.40	97 ± 290
Layer-by-layer	7.40 ± 3.58	5 ± 10	107 ± 266
Hybrid	1.64 ± 6.57	27 ± 68	9.3 ± 52.6

and this sample is slowly degraded over a period of time in the tissue. By adding PVP, the biodegradability of PCL/PVP increases compared to PCL, but this increase is uncontrollable, and the scaffold is degraded after 28 days. The degradability in the PVA/β-TCP was found to be $20\pm5\%$ after 28 days, and the biological degradation process occurs more uniformly compared to PCL/PVP. The degradation rate for layer-by-layer and hybrid scaffolds was measured $26\pm2\%$ and $40\pm5\%$, respectively, so the degradability of the scaffolds is not significantly different from each other ($p > 0.05$). The degradability properties are more related to the nature and intrinsic properties of the material. Obviously, the changes in the method have a slight effect on it, but it seems that better mechanical properties in layer-by-layer scaffold have caused less degradability than in the hybrid scaffold.

Cell viability assay

Biocompatibility and cytotoxicity are key assays to evaluate the properties of the scaffold.

Figure 5 shows the percentage of cell viability in the layer-by-layer and hybrid scaffolds, after 3, 5 and 7 days of rMSC cells culture. Layer-by-layer scaffold showed the percentage cell viability of $81\pm14\%$, $99\pm20\%$ and $95\pm7\%$ at 3, 5 and 7 days, respectively, whereas the hybrid scaffold showed cell viability of $85\pm5\%$, $84\pm3\%$ and $89\pm4\%$ at 3, 5 and 7 days, respectively, under similar experimental conditions. It seems that more hydrophilicity and better diameter distribution of the nanofibers in the layer-by-layer scaffold has made better cell viability than in hybrid nanofibers. These results demonstrate that layer-by-layer and hybrid scaffolds did not induce any cytotoxic effects on rMSC cells and they are not significantly difference from each other in cell viability ($p < 0.05$).

Fig. 4 Biodegradation of electrospun scaffolds after 28 days in PBS
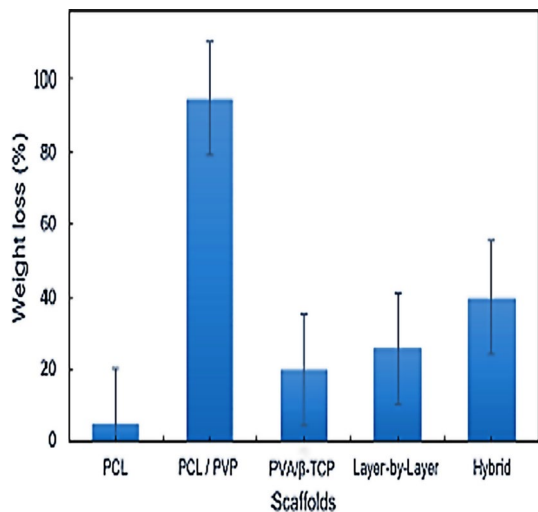
Fig. 5 Cell viability of rMSC cells cultured on layer-by-layer and hybrid electrospun scaffolds after 3, 5 and 7 days
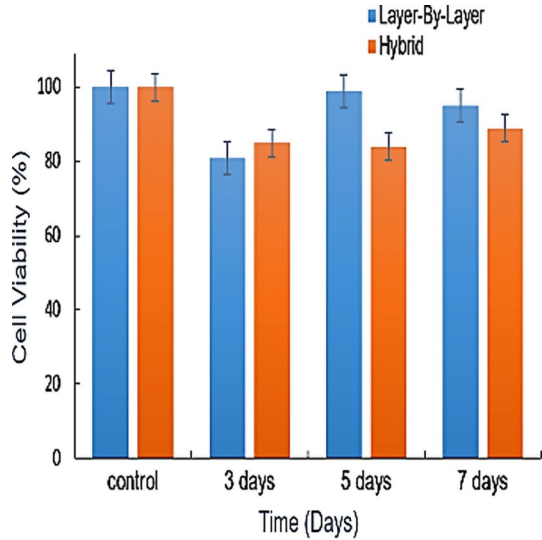

Cell morphology study

Figure 6 shows the SEM images of rMSC cells on layer-by-layer and hybrid scaffolds after 3 and 7 days of cell culture. In Fig. 6, after 3 days, the cells spread well and are connected tightly on the surfaces, demonstrating the good biocompatibility of the scaffolds. The cells get converted into spindle shape morphology in the layer-by-layer scaffold, while this morphology was not observed in the hybrid scaffold, which can be attributed to the better cell viability properties in the layer-by-layer scaffold. It is observed that the proliferation of the cells in the scaffolds increase after 7 days and the cells are densely ordered, which shows good proliferation (as shown in Fig. 6 with the red rectangle).

Conclusions

In this present study, layer-by-layer and hybrid nanofiber scaffolds were first successfully fabricated and evaluated using a combination of PCL/PVP and PVA/β-TCP layers by electrospinning method. The morphological results of layer-by-layer and hybrid scaffolds show interconnected networks without beaded morphology in the nanofibers while the mean fibers diameter related to layer-by-layer and hybrid scaffolds was measured 446 ± 128 nm and 505 ± 261 nm, respectively. FTIR spectroscopy confirms the presence of polymers and functional groups in nanoparticles in the separate layers. Hydrophilic polymers such as PVP and PVA have been used to improve the hydrophilicity and degradability of pure PCL used in the other works. The hydrophilicity of layer-by-layer and hybrid scaffolds were calculated $822 \pm 245\%$ and $560 \pm 125\%$, respectively, and the degradation rate was measured
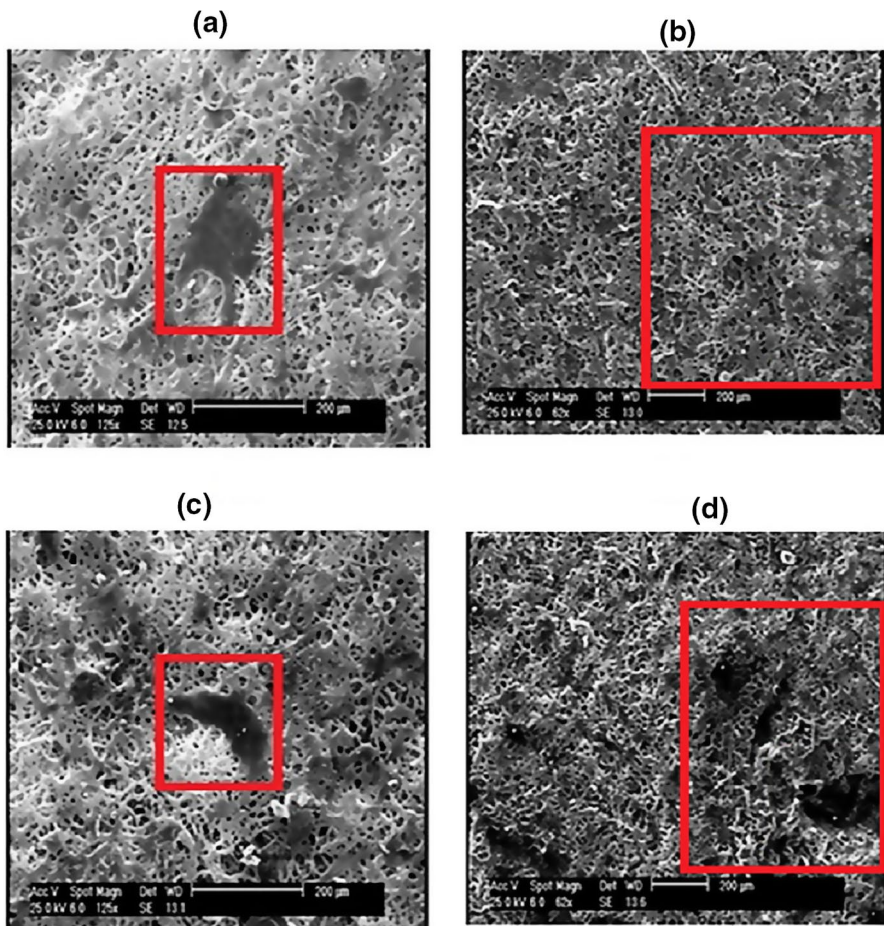
Fig. 6 SEM micrograph of rMSC cells cultured on electrospun scaffolds: **a** layer-by-layer after 3 days; **b** hybrid after 3 days; **c** layer-by-layer after 7 days and **d** hybrid after 7 days

for layer-by-layer and hybrid scaffolds $26 \pm 2\%$ and $40 \pm 5\%$, respectively. The results show improved hydrophilicity and biodegradability in both layer-by-layer and hybrid scaffolds compared to pure PCL. Mechanical properties results show that the layer-by-layer scaffold has higher tensile strength and tensile modulus and also less elongation at break than the hybrid scaffold. The reason seems to be that layer-by-layer scaffold has smaller mean fiber diameter and more uniform diameter distribution, due to the hybrid scaffold.

On the other hand, MTT assay results showed success in cell viability of the scaffolds and the absence of cell cytotoxicity for layer-by-layer and hybrid scaffolds after adding hydrophilic polymers such as PVP and PVA to pure PCL. Also, in this study, a comparison was done for the first time between the two different scaffolds fabricated. The layer-by-layer scaffold showed the percentage cell viability of $81 \pm 14\%$,

$99 \pm 20\%$ and $95 \pm 7\%$ at 3, 5 and 7 days, respectively, whereas the hybrid scaffold showed cell viability of $85 \pm 5\%$, $84 \pm 3\%$ and $89 \pm 4\%$ at 3, 5 and 7 days, respectively, under similar experimental conditions. It seems that more hydrophilicity and better diameter distribution of the nanofibers in the layer-by-layer has made better cell viability than in hybrid nanofibers. The morphology of rMSC cells on the scaffolds show the growth and proliferation of cells that are suitable for tissue engineering applications. Therefore, although layer-by-layer scaffold is more desirable than hybrid scaffold due to its smaller diameter, more uniform diameter distribution and higher hydrophilicity, both types of scaffolds can be used in several tissue engineering applications, including improvement of bone tissue regeneration.

References

1. Arafat MT, Lam CX, Ekaputra AK, Wong SY, Li X, Gibson I (2011) Biomimetic composite coating on rapid prototyped scaffolds for bone tissue engineering. Acta Biomater 7(2):809–820
2. Mohseni M, Bas O, Castro NJ, Schmutz B and Hutmacher DW (2019) Additive biomanufacturing of scaffolds for breast reconstruction. Addit Manuf 30100845.
3. Liu X, Smith LA, Hu J, Ma PX (2009) Biomimetic nanofibrous gelatin/apatite composite scaffolds for bone tissue engineering. Biomaterials 30(12):2252–2258
4. Rajzer I, Grzybowska-Pietras J, Janicki J (2011) Fabrication of bioactive carbon nonwovens for bone tissue regeneration. Fibres Text East Eur 1(84):66–72
5. Xie J, Zhong S, Ma B, Shuler FD, Lim CT (2013) Controlled biomineralization of electrospun poly (ε-caprolactone) fibers to enhance their mechanical properties. Acta Biomater 9(3):5698–5707
6. Ang SL, Shaharuddin B, Chuah JA, Sudesh K (2020) Electrospun poly (3-hydroxybutyrate-co-3-hydroxyhexanoate)/silk fibroin film is a promising scaffold for bone tissue engineering. Int J Biol Macromol 145:173–188
7. Kang Z, Zhang X, Chen Y, Akram MY, Nie J, Zhu X (2017) Preparation of polymer/calcium phosphate porous composite as bone tissue scaffolds. Mater Sci Eng C 70:1125–1131
8. Wu T, Ding M, Shi C, Qiao Y, Wang P, Qiao R, Zhong J (2020) Resorbable polymer electrospun nanofibers: History, shapes and application for tissue engineering. Chin Chem Lett 31(3):617–625
9. Daglar O, Altinkok C, Acik G, Durmaz H (2020) Electrospinning of poly (1,4-Cyclohexanedimethylene Acetylene Dicarboxylate): study on the morphology, wettability, thermal and biodegradation behaviors. Macromol Chem Phys 221(23):2000310
10. Bhattarai RS, Bachu RD, Boddu SH, Bhaduri S (2019) Biomedical applications of electrospun nanofibers: Drug and nanoparticle delivery. Pharmaceutics 11(1):5
11. Xie J, Blough ER, Wang CH (2012) Submicron bioactive glass tubes for bone tissue engineering. Acta Biomater 8(2):811–819
12. Winn SR, Hu Y, Sfeir C, Hollinger JO (2000) Gene therapy approaches for modulating bone regeneration. Adv Drug Deliv Rev 42(1–2):121–138
13. Rezwan K, Chen QZ, Blaker JJ, Boccaccini AR (2006) Biodegradable and bioactive porous polymer/inorganic composite scaffolds for bone tissue engineering. Biomaterials 27(18):3413–3431
14. Nazir NM, Dasmawati M, Azman S, Omar NS, Othman R (2012) Biocompatibility of in house β-tricalcium phosphate ceramics with normal human osteoblast cell. J Eng Sci Technol 7:169–176
15. LeGeros RZ (2008) Calcium phosphate-based osteoinductive materials. Chem Rev 108(11):4742–4753
16. Yuan H, Fernandes H, Habibovic P, De Boer J, Barradas AM, De Ruiter A, Walsh WR, Van Blitterswijk CA, De Bruijn JD (2010) Osteoinductive ceramics as a synthetic alternative to autologous bone grafting. Proc Natl Acad Sci 107(31):13614–13619

17. Boyan BD, Schwartz Z (2011) Are calcium phosphate ceramics 'smart' biomaterials? Nat Rev Rheumatol 7(1):8–9

18. He Y, Wildman RD, Tuck CJ, Christie SD, Edmondson S (2016) An investigation of the behavior of solvent based polycaprolactone ink for material jetting. Sci Rep 6:20852

19. Fabbri P, Bondioli F, Messori M, Bartoli C, Dinucci D, Chiellini F (2010) Porous scaffolds of poly-caprolactone reinforced with in situ generated hydroxyapatite for bone tissue engineering. J Mater Sci Mater Med 21(1):343–351

20. Rajzer I (2014) Fabrication of bioactive polycaprolactone/hydroxyapatite scaffolds with final bilayer nano-/micro-fibrous structures for tissue engineering application. J Mater Sci 49(16):5799–5807

21. Cima LG, Vacanti JP, Vacanti C, Ingber D, Mooney D, Langer R (1991) Tissue engineering by cell transplantation using degradable polymer substrates. ASME J Biomech Eng 113(2):143–151

22. Vaz CM, Van Tuijl S, Bouten CVC, Baaijens FPT (2005) Design of scaffolds for blood vessel tissue engineering using a multi-layering electrospinning technique. Acta Biomater 1(5):575–582

23. Chong EJ, Phan TT, Lim IJ, Zhang YZ, Bay BH, Ramakrishna S, Lim CT (2007) Evaluation of electrospun PCL/gelatin nanofibrous scaffold for wound healing and layered dermal reconstitution. Acta Biomater 3(3):321–330

24. Chung TW, Cho KY, Lee HC, Nah JW, Yeo JH, Akaike T, Cho CS (2004) Novel micelle-forming block copolymer composed of poly (ε-caprolactone) and poly (vinyl pyrrolidone). Polymer 45(5):1591–1597

25. Kim CH, Khil MS, Kim HY, Lee HU, Jahng KY (2006) An improved hydrophilicity via electrospinning for enhanced cell attachment and proliferation. J Biomed Mater Res Part B Appl Biomater 78(2):283–290

26. Jia YT, Zhu XY, Liu QQ (2011) In vitro degradation of electrospun fiber membranes of PCL/PVP blends. Adv Mater Res 332:1330–1334

27. Li J, Zhang L, Gu J, Sun Y, Ji X (2015) Cross-linking of poly (vinyl alcohol) with N, N′-methylene bisacrylamide via a radical reaction to prepare pervaporation membranes. RSC Adv 5(26):19859–19864

28. Ding B, Kim HY, Lee SC, Shao CL, Lee DR, Park SJ, Kwag GB, Choi KJ (2002) Preparation and characterization of a nanoscale poly (vinyl alcohol) fiber aggregate produced by an electrospinning method. J Polym Sci Part B Polym Phys 40(13):1261–1268

29. Hajir Bahrami, AGKS, Kochaksaraie AS (2012) Morphological, mechanical and biological properties of novel PCL-Cs/PVA multi layer nanofibrous scaffolds. Dig J Nanomater Biostructures 7(4)

30. Meng ZX, Wang YS, Ma C, Zheng W, Li L, Zheng YF (2010) Electrospinning of PLGA/gelatin randomly-oriented and aligned nanofibers as potential scaffold in tissue engineering. Mater Sci Eng C 30(8):1204–1210

31. Amiraliyan N, Nouri M, Kish MH (2009) Effects of some electrospinning parameters on morphology of natural silk-based nanofibers. J Appl Polym Sci 113(1):226–234

32. Çakman G, Dilsiz N (2016) Preparation and physical, thermal properties of polycaprolactone/m-Halloysite nanocomposite. J Multidiscip Eng Sci Stud 2:842–848

33. Zhou Y, Yang D, Chen X, Xu Q, Lu F, Nie J (2008) Electrospun water-soluble carboxyethyl chitosan/poly (vinyl alcohol) nanofibrous membrane as potential wound dressing for skin regeneration. Biomacromol 9(1):349–354

34. Zhang JF, Yang DZ, Xu F, Zhang ZP, Yin RX, Nie J (2009) Electrospun core−shell structure nanofibers from homogeneous solution of poly (ethylene oxide)/chitosan. Macromolecules 42(14):5278–5284

35. Kai D, Low ZW, Liow SS, Abdul Karim A, Ye H, Jin G, Li K, Loh XJ (2015) Development of lignin supramolecular hydrogels with mechanically responsive and self-healing properties. ACS Sustain Chem Eng 3(9):2160–2169

36. Yang D, Zhang J, Xue J, Nie J, Zhang Z (2013) Electrospinning of Poly (3-hydroxybutyrate-co-3-hydroxyvalerate) nanofibers with feature surface microstructure. J Appl Polym Sci 127(4):2867–2874

37. Li Q, Yang D, Ma G, Xu Q, Chen X, Lu F, Nie J (2009) Synthesis and characterization of chitosan-based hydrogels. Int J Biol Macromol 44(2):121–127

38. Esfahani H, Salahi E, Tayebifard SA, Rahimipour MR, Keyanpour-Rad M (2014) Synthesis of polycaprolactam/zinc doped hydroxyapatite nanofibers via electrospinning. J Adv Mater Technol 3(3):59–66

39. Giannitelli SM, Costantini M, Basoli F, Trombetta M and Rainer A (2018) Electrospinning and microfluidics: An integrated approach for tissue engineering and cancer. In: Electrofluidodynamic

technologies (EFDTs) for biomaterials and medical devices. Woodhead Publishing Series in Bioma-terials, pp 139–155

40. Maheshwari SU, Samuel VK, Nagiah N (2014) Fabrication and evaluation of (PVA/HAp/PCL) bilayer composites as potential scaffolds for bone tissue regeneration application. Ceram Int 40(6):8469–8477

41. Ma G, Yang D, Wang K, Han J, Ding S, Song G, Nie J (2010) Organic-soluble chitosan/polyhy-droxybutyrate ultrafine fibers as skin regeneration prepared by electrospinning. J Appl Polym Sci 118(6):3619–3624

42. Karageorgiou V, Kaplan D (2005) Porosity of 3D biomaterial scaffolds and osteogenesis. Biomateri-als 26(27):5474–5491

43. Gönen SÖ, Taygun ME, Küçükbayrak S (2016) Fabrication of bioactive glass containing nanocom-posite fiber mats for bone tissue engineering applications. Compos Struct 138:96–106

Authors and Affiliations

Majid Sohrabi[1] · Marjan Abbasi[1] · Malek Masoud Ansar[2] · Bahram Soltani Tehrani[3]

1   Department of Textile Engineering, Faculty of Engineering, University of Guilan, Rasht, Iran

2   Department of Anatomy, Cellular and Molecular Research Center, School of Medicine, Guilan University of Medical Sciences, Rasht, Iran

3   Department of Pharmacology, Cellular and Molecular Research Center, School of Medicine, Guilan University of Medical Sciences, Rasht, Iran